MAGNETIC RESONANCE IN CHEMISTRY
Magn. Reson. Chem. **36**, 706–714 (1998)

Pulse sequences for high-resolution diffusion-ordered spectroscopy (HR-DOSY)¶

Michelle D. Pelta,[1] Hervé Barjat,[1]† Gareth A. Morris,[1]* Adrian L. Davis[2]‡ and Stephen J. Hammond[2]

[1] Department of Chemistry, University of Manchester, Oxford Road, Manchester M13 9PL, UK
[2] Shell Research Limited, SRTCT, P.O. Box 1, Chester CH1 3SH, UK

Received 9 March 1998; revised 1 May 1998; accepted 1 May 1998

ABSTRACT: Six pulse sequences are described, all based on the stimulated echo, for use in high resolution diffusion-ordered spectroscopy (HR-DOSY). HR-DOSY requires spectra with clean baselines, pure phases and lineshapes that are independent of field gradient pulse amplitude. Lineshape problems arising from the static field perturbations caused by field gradient pulses and phase errors caused by zero quantum coherence in strongly coupled spin systems are discussed, and the performance of the six sequences is compared. Pulse sequences which use balanced pairs of antiphase field gradient pulses show significant advantages. © 1998 John Wiley & Sons Ltd.

KEYWORDS: NMR; DOSY; stimulated echo; bipolar pulse sequences; zero quantum coherence

INTRODUCTION

Diffusion-ordered spectroscopy (DOSY)[1–11] seeks to separate the NMR signals of different species according to their diffusion coefficients. A series of spin-echo spectra are measured with different pulsed field gradient strengths, and the signal decays are analysed to extract a set of diffusion coefficients with which to synthesize the diffusion domain of a DOSY spectrum. In 2D DOSY the initial diffusion-weighted spectra are one-dimensional; adding diffusion weighting to 2D experiments such as COSY, NOESY or HMQC gives 3D DOSY[12–17] spectra. DOSY can be roughly subdivided into two areas: low-resolution DOSY,[1–7] of simple mixtures of molecules with widely differing sizes and poorly resolved NMR spectra, and high-resolution DOSY (HR-DOSY),[8–11] of more complex mixtures which may contain molecules of very similar sizes but which give well resolved NMR spectra. The difficulty of extracting clean diffusion parameters from overlapping signal decays sets strict limits on the diffusion resolution of low-resolution DOSY, but in the high-resolution case relatively small differences (of the order of 1%) in diffusion coefficient can be resolved. To identify such small differences reliably it is necessary that the systematic errors be reduced to an absolute minimum: the challenge of designing successful HR-DOSY techniques is to combine experimental methods which minimize such errors with data analysis procedures which compensate as accurately as possible for the errors that remain. This paper is primarily concerned with evaluating the impact of systematic errors with six different pulse sequences, three of which have been described previously and three of which have not.

In HR-DOSY the simplifying assumption is generally made that each peak in the NMR spectrum corresponds to a single species; fitting the decay of the height of each peak as a function of the square of field gradient pulse area to a single exponential then yields a diffusion coefficient and a standard error for each signal in the NMR spectrum. The diffusion dimension of the DOSY spectrum is synthesized by placing a Gaussian signal in the diffusion domain for each peak in the NMR spectrum. The Gaussian is centred on the fitted diffusion coefficient, has a width proportional to the standard error obtained from the fitting process, and is of volume or amplitude proportional to the initial NMR peak height. The best relative accuracy in diffusion coefficient is obtained if a two-parameter (initial amplitude and decay constant) fit is used, but this requires that all signals decay towards zero, and therefore makes maintenance of a clean spectral baseline important. The effect of any baseline offsets is to bias the decay constants and to degrade the standard errors obtained. Care should therefore be taken to use experimental conditions (e.g. acquisition timing, choice of analogue filter bandwidth) that give flat baselines, and after initial Fourier transformation it may be helpful to apply baseline correction. It is also important to ensure that all signals have pure absorption phase. Even small phase errors can have significant effects, since the broad tails of dispersion mode signals extend far further than the skirts of an absorption mode lineshape. The dispersion tails have two undesirable effects: they greatly increase

* Correspondence to: G. A. Morris, Department of Chemistry, University of Manchester, Oxford Road, Manchester M13 9PL, UK
E-mail: g.a.morris@man.ac.uk
† Present address: University Chemical Laboratory, Lensfield Road, Cambridge CB2 1EW, UK.
‡ Present address: Pfizer Central Research, Sandwich, Kent CT13 9NJ, UK.
¶ Dedicated to Professor John D. Roberts on the occasion of his 80th birthday.
Contract/grant sponsor: EPSRC; *Contract/grant number:* GR/K16296; *Contract/grant number:* GR/K44619; *Contract/grant number:* GR/L 17443.

CCC 0749-1581/98/100706–09 $17.50

the probability of significant signal overlap, and hence of cross-contamination of decay curves, and they interfere with the proper correction of baseline errors.

There are some clear objections to the very simple approach to HR-DOSY outlined above. Real spectra are very rarely completely resolved, making some degree of error in the apparent diffusion coefficients almost inevitable. Unless two overlapping signals have very different diffusion coefficients, the effect of the mixing of their decay curves on the standard error of the fit will be relatively small, while the diffusion coefficient obtained will be a compromise value. The misleading result is then an apparently well defined diffusion peak at an unrealistic diffusion coefficient. Applying baseline correction to remove baseline errors represents a significant falsification of the experimental data, since some real signal is subtracted along with the errors. These objections have some force but, as with any spectroscopic tool, the most important criteria are the quality of the information obtainable and the ease with which that information can be obtained. HR-DOSY spectra do indeed give misleading results where signals overlap, but this is immediately obvious from the spectrum (i.e. the signals are adjacent or unresolved in the NMR domain) and straightforward to interpret: the composite peak from two overlapping signals will appear in an HR-DOSY spectrum at a diffusion coefficient intermediate between the diffusion coefficients of the two isolated signals. Real signals are indeed subtracted along with baseline errors, but this does not affect the decay of the apparent signal amplitude: baseline correction properly applied should always improve the accuracy of the diffusion coefficients obtained.

It is instructive to examine the merits of a more sophisticated approach, placing less reliance on the skill of the experimenter in interpreting DOSY data. Relaxing the requirement that each peak in the NMR spectrum be interpreted as having a single decay constant immediately degrades the certainty of the diffusion coefficients obtained very substantially: unless the input data are of extremely (and generally unrealistically) high purity and signal-to-noise ratio, the standard errors obtained even for single decays will be much larger than those obtained from a two-parameter fit. If baseline correction is not used, then in all but the simplest spectra the cumulative effect of overlapping skirts of absorption mode lineshapes will be to distort all the peak height decay curves through cross-talk, again degrading the accuracy of fitting. A stricter approach to this problem and to the overlap problem in general would be to fit the entire spectral bandshape rather than just the peak maxima, but this begs the question of how to factorize the initial spectrum into bandshapes for individual species, and would increase the computing resources required by orders of magnitude. Thus far at least it would appear that the simple HR-DOSY analysis outlined above is the method of choice for DOSY analysis of mixtures of small molecules.

The first criterion for a successful DOSY pulse sequence is that it should give absorption mode signals. This strongly favours stimulated echo[18] over Carr–Purcell pulse sequences,[19] because of the need to minimize J modulation. The basic Carr–Purcell $90°$–τ–$180°$–τ– pulse sequence with field gradient pulses applied immediately after the $90°$ pulse and immediately before data acquisition has the virtue that all of the available NMR signal is acquired, but in the presence of homonuclear scalar coupling the delays τ must be kept small compared with $1/J$ if phase errors on multiplet components are to be avoided. In proton NMR this makes the diffusion period 2τ unrealistically small with the field gradient pulse amplitudes normally available. Even in systems with no scalar coupling, T_2 losses may make the Carr–Purcell sequence unattractive. The merit of the basic stimulated echo sequence $90°$–τ–$90°$–Δ–$90°$–τ– is that the delays τ during which the magnetization is transverse to the main field need only be long enough to enclose field gradient pulses, while the (spatially encoded) magnetization is longitudinal during the diffusion period Δ. Only half of the signal survives to be acquired in the stimulated echo, but J modulation and relaxation losses are kept to a minimum.

In most cases the simple stimulated echo pulse sequence with short τ delays does give pure absorption mode signals. There is, however, one set of circumstances in which significant phase errors do occur, even in the ideal case of perfect pulses and infinitely short τ delays. Anomalies are visible when long diffusion delays Δ are used with some spin systems showing second-order effects, for example AB spin systems. Approximately equal and opposite phase errors are seen for the multiplets of the two coupled groups. In AB systems with a relatively small degree of strong coupling it is clear that the phase errors are the same within the A multiplet and equal and opposite to those in the B multiplet (as can be seen in some of the spectra in Fig. 2). This is in contrast to the effects of J modulation, where the phase errors are opposite within a given multiplet and equal to those in the other. These strong coupling phase anomalies occur when the relaxation of zero quantum coherence during the diffusion delay is slower than that of longitudinal magnetization, and disappear for short diffusion times. The effect was first described in proton stimulated echo measurements on citrate *in vivo*,[20] and has been extensively analysed. As will be seen below, the phase anomalies can be eliminated if the pulse sequence is amended to avoid the excitation of zero quantum coherence.

The second main criterion for a successful DOSY sequence is that it should minimize perturbation of the measurement of the NMR signal by the after-effects of field gradient pulses. The substantial disturbances of the static field needed for the measurement of diffusion in NMR spectroscopy inevitably take some time to subside. Finite gradient pulse fall times, eddy currents induced in probe and magnet metalwork, coupling between the gradient coil and the main magnetic field and disturbance of the field-frequency lock system all combine to degrade the NMR lineshape. Since the extent of the degradation increases with the amplitude

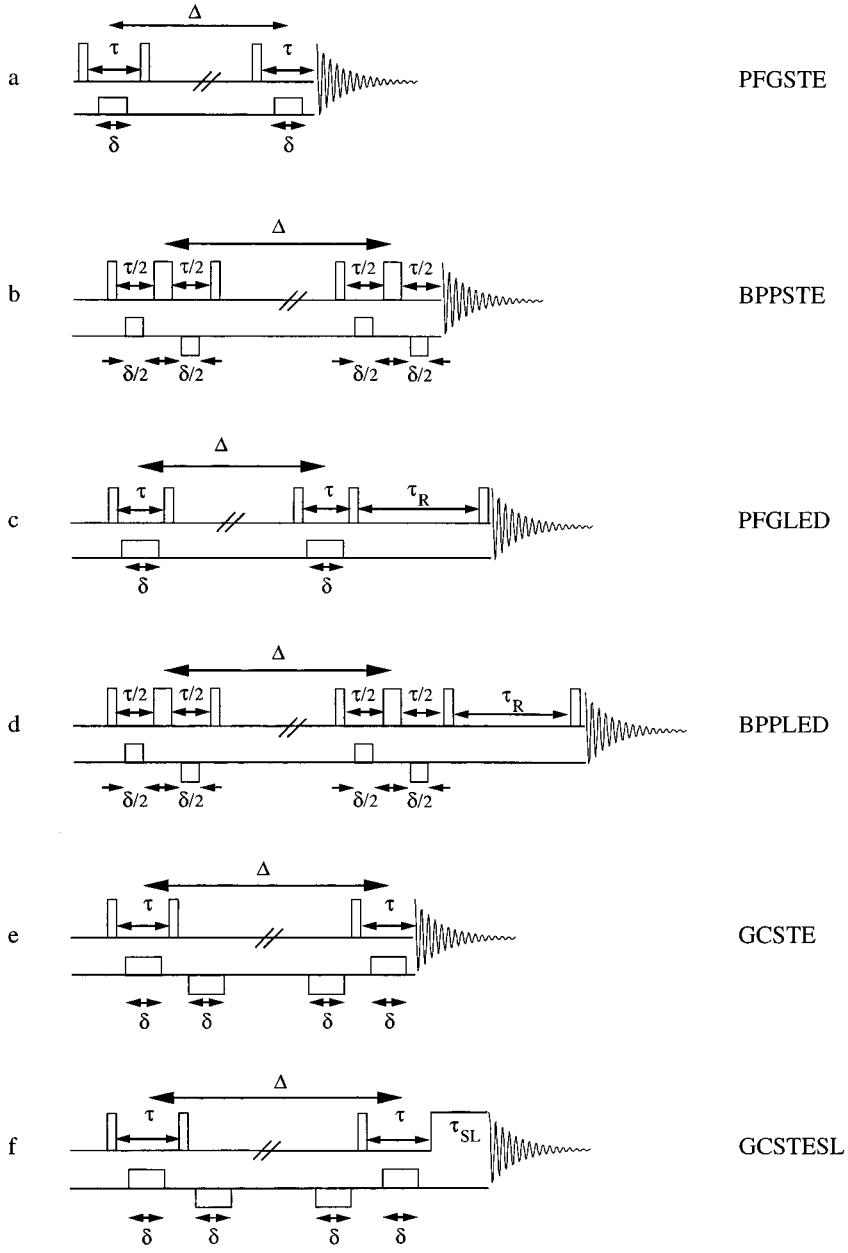

Figure 1. Pulse sequences for HR-DOSY, each showing (top) proton and (bottom) *z* gradient channel: (a) pulsed field gradient stimulated echo, PFGSTE; (b) bipolar pulse pair stimulated echo, BPPSTE; (c), pulsed field gradient longitudinal eddy delay, PFGLED; (d) bipolar pulse pair longitudinal eddy delay, BPPLED; (e) gradient compensated stimulated echo, GCSTE; and (f) gradient compensated stimulated echo spin lock, GCSTESL.

and the duration of the field gradient pulses, the decay in the peak height of an NMR signal that results as the field gradient pulse area is increased is faster than expected from diffusion alone, and unless precautions are taken the effect will be to increase apparent diffusion coefficients and increase the errors estimated from the fitting process.

The introduction of actively shielded field gradient probe systems[21] into high-resolution NMR has greatly reduced the damage done by gradient pulses, but even with the best available equipment the lineshape perturbations that result from incorporating gradient pulses into the basic stimulated echo sequence are still sufficient to degrade DOSY spectra substantially. It is therefore important to design sequences so that the field perturbation during data acquisition is minimized. Post-processing of the experimental data, using reference deconvolution[22] to correct the lineshape distortions, can also be used to reduce further the impact of lineshape variation with field gradient pulse area. The two expedients that have been used most commonly are to add a polarization storage delay to the end of a sequence, to allow the field perturbations to decay, and to use bipolar field gradient pulse pairs. Two new sequences are introduced here which use the latter technique without the need for extra 180° refocusing pulses. Bipolar pulse pair techniques have the added advantage of refocusing both B_0 inhomogeneity and chemical shifts; the latter can be important in strongly coupled spin systems, as will be seen below.

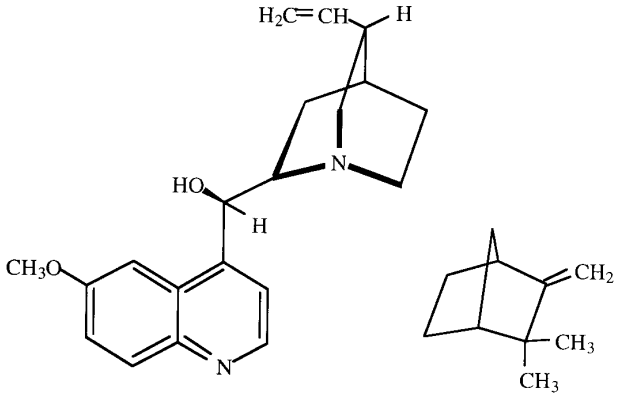

1 3

$(CH_3)_2C{=}CHCH_2CH_2C(CH_3){=}CHCH_2OH$

2

The six pulse sequences examined here, and illustrated in Fig. 1, are the basic stimulated echo sequence with field gradient pulses [PFGSTE, Fig. 1(a)]; the Bipolar Pulse Pair STimulated Echo pulse sequence [BPPSTE, Fig. 1(b)], in which bipolar field gradient pulse pairs[23] bracketing 180° refocussing pulses replace the simple field gradient pulses of PFGSTE; the Pulsed Field Gradient Longitudinal Eddy Delay pulse sequence [PFGLED, Fig. 1(c)], in which a polarization storage delay for field recovery τ_R is added to the PFGSTE sequence; the Bipolar Pulsed Field Gradient Longitudinal Eddy Delay pulse sequence[24] [BPPLED, Fig. 1(d)], which combines PFGLED with BPPSTE (the BPPSTE sequence does not appear to have been described explicitly in the literature, but is implicit in the BPPLED sequence of Wu, Chen and Johnson); the Gradient Compensated Stimulated Echo pulse sequence [GCSTE, Fig. 1(e)], which places the antiphase gradient pulses within the diffusion delay and hence does away with the need for 180° pulses; and the Gradient Compensated Stimulated Echo Spin Lock pulse sequence [GCSTESL, Fig. 1(f)], which adds a spin lock purge pulse of duration τ_{SL} to GCSTE.

Table 1. Phase cycling for the GCSTE sequence[a]

ϕ_1	0213
ϕ_2	$(0_8 2_8)_2\ (1_8 3_8)_2$
ϕ_3	$(0_4 2_4)_2\ (1_4 3_4)_2$
ϕ_R	$\phi_2 + \phi_3 - \phi_1$

[a] Pulse phases are shown in order of appearance, with receiver phase ϕ_R. Phase shifts are indicated in multiples of 90°, with subscripts indicating repetition; thus $(0_4 2_4)_2$ indicates the sequence 0° 0° 0° 0° 180° 180° 180° 180° 0° 0° 0° 0° 180° 180° 180° 180°.

Table 2. Phase cycling for the GCSTESL sequence[a]

ϕ_1	0213
ϕ_2	$(0_8 2_8)_2\ (1_8 3_8)_2$
ϕ_3	$(0_4 2_4)_2\ (1_4 3_4)_2$
ϕ_4	$13 + 0_{64} 2_{64} + \phi_2 + \phi_3 - \phi_1$
ϕ_R	$\phi_2 + \phi_3 - \phi_1$

[a] Pulse phases are shown in order of appearance, with receiver phase ϕ_R. Phase shifts are denoted as in Table 1.

Table 3. Phase cycling for the BPPSTE sequence[a]

ϕ_1	0202 1313
ϕ_2	0
ϕ_3	0
ϕ_4	$(0022)_2(1133)_2(2200)_2(3311)_2$
ϕ_5	$0_8 2_8$
ϕ_R	$\phi_1 + 2\phi_5 - \phi_4 + (\phi_3 - 2\phi_2)$

[a] Pulse phases are shown in order of appearance, with receiver phase ϕ_R. Phase shifts are denoted as in Table 1.

EXPERIMENTAL

All six pulse sequences were implemented on a Varian Unity INOVA 400 narrow bore spectrometer equipped with a Performa II gradient pulse amplifier and an actively shielded 5 mm indirect detection probe capable of producing up to 30 G cm^{-1} z field gradient pulses. The sample used consisted of a mixture of quinine (**1**), geraniol (**2**) and camphene (**3**) in deuteromethanol, with TMS as reference material. All experiments were carried out at room temperature with a static sample. Automated z gradient shimming based on deuterium spin echoes was used.[25] Experimental conditions were chosen to emphasize different aspects of sequence performance. All the pulse sequences used phase cycling designed to enforce the stimulated echo coherence transfer pathway; the phase cycles for the recommended sequences, GCSTE, GCSTESL and BPPSTE, are listed in Tables 1–3. No gradient pulses were used in the diffusion delay.

RESULTS

Figure 2 compares the results of applying the sequences of Fig. 1 to the mixture sample, using two distinct sets of experimental conditions. All signals are shown with a large vertical expansion, to enable any phase and lineshape errors to be seen more clearly. Traces a–f (left) show the aromatic region of the spectrum, which includes the quinine ABC system with multiplets at 7.39 (AB) and 7.96 (C) ppm, and were recorded with a long diffusion time Δ of 0.8 s, a diffusion-encoding gradient pulse width τ of 1 ms and a relatively modest gradient strength of 1 G cm^{-1}. The recovery time τ_R for traces c and d was 50 ms. Under these conditions the slightly slower relaxation of the zero quantum coherence in the AB spin system compared with that of longitudinal magnetization leads to the appearance of phase anomalies on the ABC signals in the normal stimulated echo experiment (trace a), and in the PFGLED (trace c) and GCSTE (trace e) experiments. In the BPPSTE and BPPLED sequence (traces b and d), the refocusing

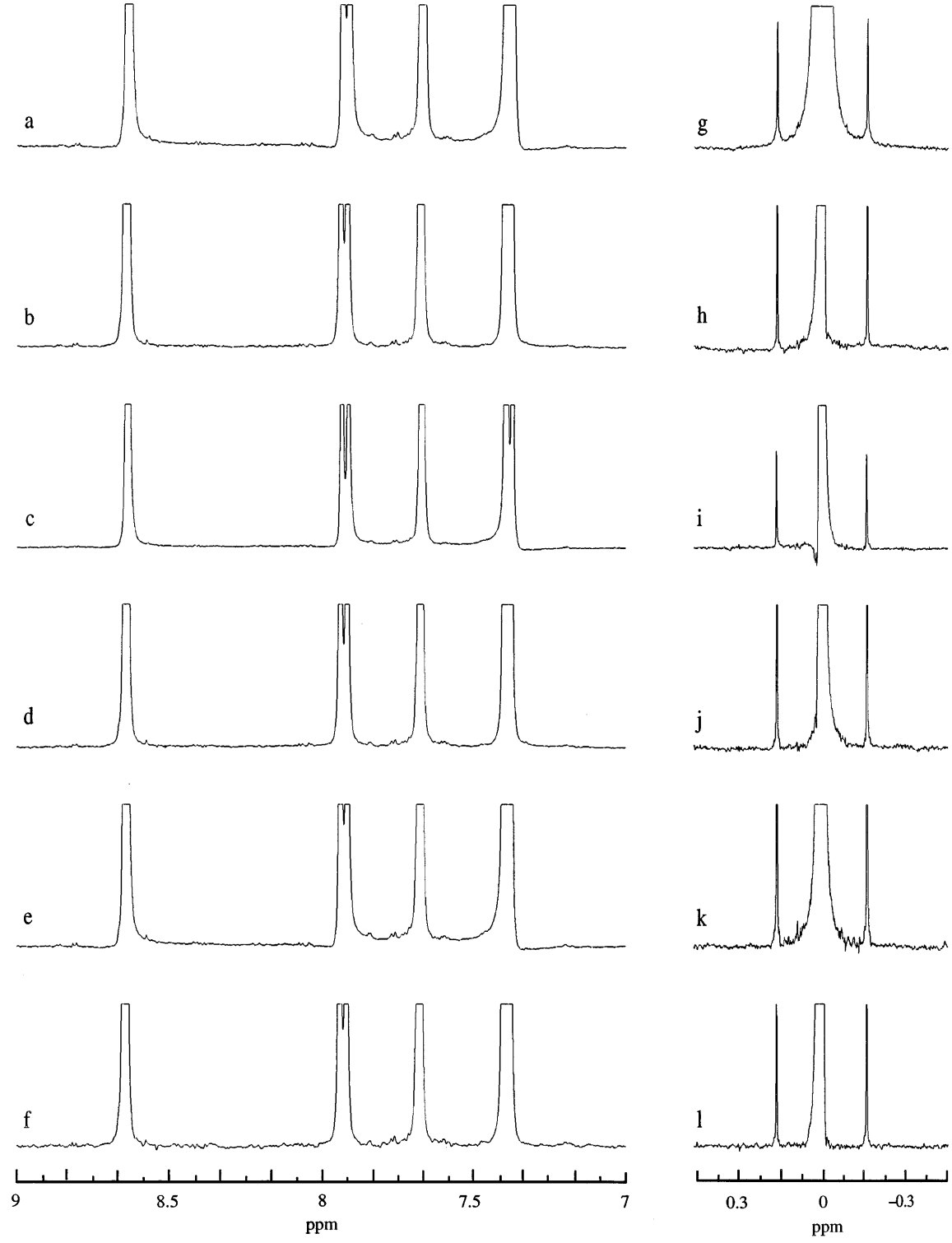

Figure 2. 400 MHz proton spectra of a mixture of quinine (**1**), geraniol (**2**) and camphene (**3**) in deuteromethanol, with TMS as reference material. Left, (a)–(f), aromatic region, recorded with pulse sequences in Fig. 1(a)–(f) using a diffusion delay Δ of 0.8 s, diffusion-encoding gradient pulse widths δ of 1 ms and a field gradient strength of 1 G cm^{-1}. The sequences in Fig. 1(c) and (d) used a recovery delay τ_R of 50 ms and the sequence in Fig. 1(f) a spin-lock time of 1.5 ms with 64 transients. Right, (g)–(l), TMS region of the same mixture, obtained with pulse sequences in Fig. 1(a)–(f) using a diffusion delay Δ of 0.2 s, diffusion-encoding gradient pulse widths δ of 2 ms [1 + 1 ms for the sequences in Fig. 1(b) and (d)]. The sequences in Fig. 1(c) and (d) used a recovery delay τ_R of 50 ms and the sequence in Fig. 1(f) a spin-lock time of 1.5 ms with 64 transients.

action of the 180° pulses suppresses the effect of chemical shifts during the τ delays, so that antiphase single quantum coherence is not converted into zero quantum. In the GCSTESL sequence of [Fig. 1(f)], the phase anomalies are suppressed by a spin lock purge pulse (Fig. 2, trace f).

Traces g–l in Fig. 2 (right) show the TMS region of the spectrum at high vertical expansion, recorded with a

diffusion delay Δ of 20 ms, a diffusion-encoding gradient pulse width τ of 2 ms and a strong gradient strength of 30 G cm^{-1}. These conditions illustrate the damage that can be done by strong gradient pulses even using a probe with very good active shielding. The simple stimulated echo (trace g) shows severe broadening of the base of the TMS line, caused by the recovery of B_0 homogeneity during the first few milliseconds of the acquired signal. Adding a polarization storage period τ_R to give the PFGLED sequence circumvents this problem, only to reveal the less tractable sharp lineshape disturbance shown in trace i. This arises from longer lived B_0 disturbances, including those caused by the perturbation of the deuterium field-frequency lock. To extend τ_R sufficiently to eliminate this source of lineshape error would be to degrade the sensitivity of the experiment unacceptably.

The best lineshape results are obtained from those experiments (BPPSTE, BPPLED, GCSTE and GCSTESL) where matched pairs of field gradient pulses of opposite sign are used. The two principal reasons for this are the first order cancellation of the B_0 field and field homogeneity perturbations that follow the gradient pulses, and the much smaller perturbation of the deuterium lock signal that such bipolar pulse pairs give. Since the deuterium signals do not experience the 180° proton pulses, the effects of the adjacent positive and negative gradient pulses cancel to give a deuterium gradient echo, and the net result is only a very slight hiatus in the lock signal. Since the feedback loop of typical field-frequency lock system has a time constant in the range 1–40 s, the longer term ($>$ 5 ms) effect of the gradient pulse pairs on field stability (and hence on lineshape) is small.

The lineshapes obtained with BPPSTE (trace h) and BPPLED (trace j) are very similar; since the latter sequence requires longer phase cycling and gives slightly reduced sensitivity, the former is the preferred option on spectrometer systems such as that used here. The simpler GCSTE sequence gives a similarly acceptable lineshape, but as trace e shows, it can give phase anomalies in strongly coupled spin systems. The best lineshape is obtained using the GCSTESL sequence; this shares the advantages of the bipolar and GCSTE sequences in cancelling most of the undesirable aftereffects of the field gradient pulses, but the spin lock pulse τ_{SL} used to purge the out-of-phase components of the strongly coupled multiplets (trace f) has the added bonus of selecting a slightly more homogeneous sample volume (at surprisingly little cost in sensitivity) through the action of B_1 inhomogeneity.

DISCUSSION

The results in Fig. 2 prompt some fairly straightforward recommendations. There is a clear advantage of sequences that use antiphase gradient pulse pairs, whether bracketing 180° pulses as in the BPPSTE and BPPLED sequences [Fig. 1(b) and d)] or simply included in the diffusion delay Δ as in GCSTE and GCSTESL [Fig. 1(e) and (f)]. On spectrometers with good gradient recovery the addition of a polarization storage delay, as in the LED and BPPLED sequences [Fig. 1(c) and (d)] brings little or no benefit; such sequences may, however, be valuable on instruments with very high maximum gradient strengths, where the potential for field perturbations is much greater.

Sequences such as BPPSTE and BPPLED which use bipolar pulse pairs for diffusion encoding do have one serious constraint on their use. Since the diffusion encoding relies on the action of the 180° pulses, without which the effects of the two gradient pulses would simply cancel, it is essential that phase cycling be used to ensure that only signals which are refocused by the 180° pulses survive. This increases the minimum acceptable phase cycle 16-fold if 90° phase shifts are used, or ninefold if the most economical phase cycle, that using 120° phase shifts,[26] is employed. Skimping on the phase cycle would result in significant amounts of signal surviving the sequence independent of the gradient strength, and hence to systematic errors in the apparent diffusion coefficients obtained. Phase cycling can be a significant issue in diffusion experiments because of the need to ensure that all the spins contributing to the measured signal encounter the full diffusion weighting, i.e. follow the desired stimulated echo coherence transfer pathway. One way to reduce the phase cycle slightly is to use a field gradient pulse during the diffusion delay to suppress coherences of higher than zero order, but this would require a gradient pulse significantly larger than the largest diffusion-encoding pulse in order to avoid the refocusing of unwanted signal, and would lead to increased problems with lineshapes.

Bipolar sequences do, however, have one important advantage which is not apparent in the experimental results shown here, but which only appears in systems which have complex spin systems in large molecules. If the simple stimulated echo sequence of Fig. 1(a), or a variant such as GCSTE or GCSTESL [Fig. 1(e) or (f)] is applied to a macromolecule such as a protein, the signal loss as the diffusion delay Δ is increased, even for modest gradient strengths, is considerably greater than that expected given the spin–lattice relaxation times involved. The signal is lost through spin diffusion, the exchange of longitudinal magnetization between spins with different chemical shifts in the same molecule (as opposed to physical diffusion, where a given spin travels through the sample). Since the proton chemical shifts act during the τ delay, in addition to the magnitude and sign of the longitudinal magnetization during the diffusion delay Δ depending on position along the gradient-encoding axis, they also depend on chemical shift. Exchange of magnetization between different sites on a molecule (cross-relaxation or spin diffusion) then results in destructive interference and an averaging of the net magnetization to zero. Bipolar sequences, however, refocus the chemical shift, and as a result spin diffusion within the molecule simply exchanges magnetizations which have the same sign. There is thus overall a clear

preference for the BPPSTE sequence where spin systems which are out of extreme narrowing are involved.

The principal virtues of the GCSTE and GCSTESL sequences [Fig. 1(e) and (f)] are simplicity and economy of phase cycling. For mixtures of small molecule systems, where spin diffusion is not a problem and sensitivity can be very good, the short minimum phase cycles probably make GCSTE the pulse sequence of choice for systems which do not show strong coupling, and GCSTESL for systems which do. The BPPSTE sequence also shows very good performance for small molecule systems, but has a long minimum phase cycle and is therefore only competitive where a poor signal-to-noise ratio necessitates extensive time averaging.

The practical significance of the differences between the various pulse sequences described here is illustrated in Figs 3–5, which show 2D DOSY spectra obtained using different experimental and data processing methods. Figure 3 shows the DOSY spectrum of the mixture, obtained using the PFGSTE sequence of Fig. 1(a); no attempt was made in the construction of the DOSY spectrum to compensate for the deficiencies of the experimental data. The DOSY spectrum was thus obtained by simple Fourier transformation of the experimental signals, followed by peak picking, fitting of the peak heights to exponentials as a function of the square of the field gradient pulse area and synthesis of the DOSY spectrum. This spectrum shows broad signals in the diffusion domain, as evidenced by the poorly resolved projection on the diffusion axis, which shows considerable signal strength lying between the 'true' diffusion values for the quinine, camphene and geraniol components. The poor accuracy obtained in the diffusion domain and the spread of diffusion values are the results of the lineshape and baseline errors discussed previously. Figure 4 shows the result of applying the same simple processing method to data acquired with the GCSTESL sequence of Fig. 1(f). These data show a significant improvement in the accuracy of the diffusion values obtained for the three main components, and also a reduction in the number of signals at intermediate diffusion values. The improvement is due entirely to the reduction in lineshape errors afforded by the gradient compensated pulse sequence (GCSTE).

Figure 5 shows the DOSY spectrum obtained from the same GCSTESL data as Fig. 4, but using a more complex data processing protocol designed to reduce the impact of the experimental imperfections in the data acquired. The raw experimental data were first processed by reference deconvolution, using the TMS signal in each dataset as a reference, with a target ideal instrumental lineshape of a 0.6 Hz wide Gaussian. Regions of baseline free of signal in the first spectrum were identified manually, and baseline correction was

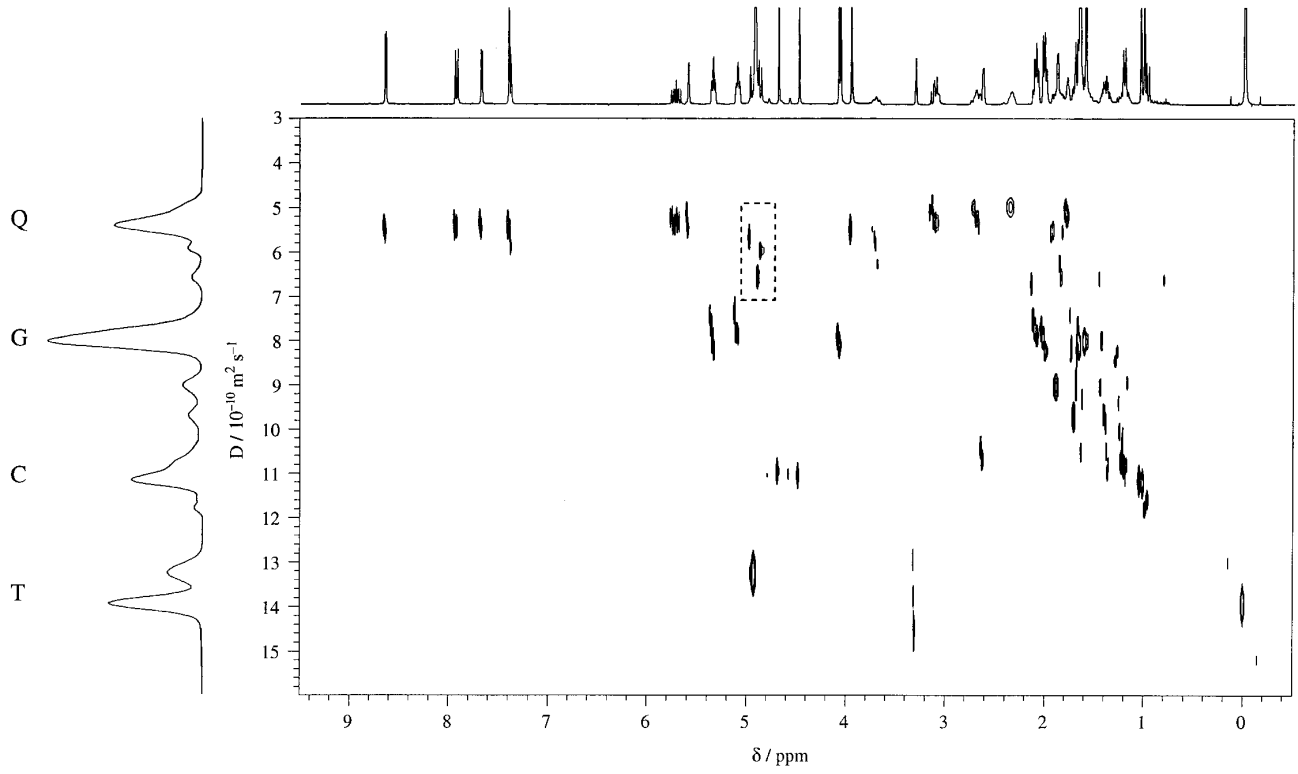

Figure 3. 400 MHz proton DOSY spectrum of the mixture used for Fig. 2, obtained using the basic stimulated echo PFGSTE sequence of Fig. 1(a), with (top) the normal 1D spectrum and (left) the integral projection of the DOSY spectrum on the diffusion axis. The labels Q, C and G indicate the signals of quinine, camphene and geraniol, respectively, and T the solvent and TMS signals. The dotted box highlights the region around 4.9 ppm referred to in the text. The simple DOSY spectrum synthesis algorithm used, described in the text, makes no attempt to correct for experimental imperfections.

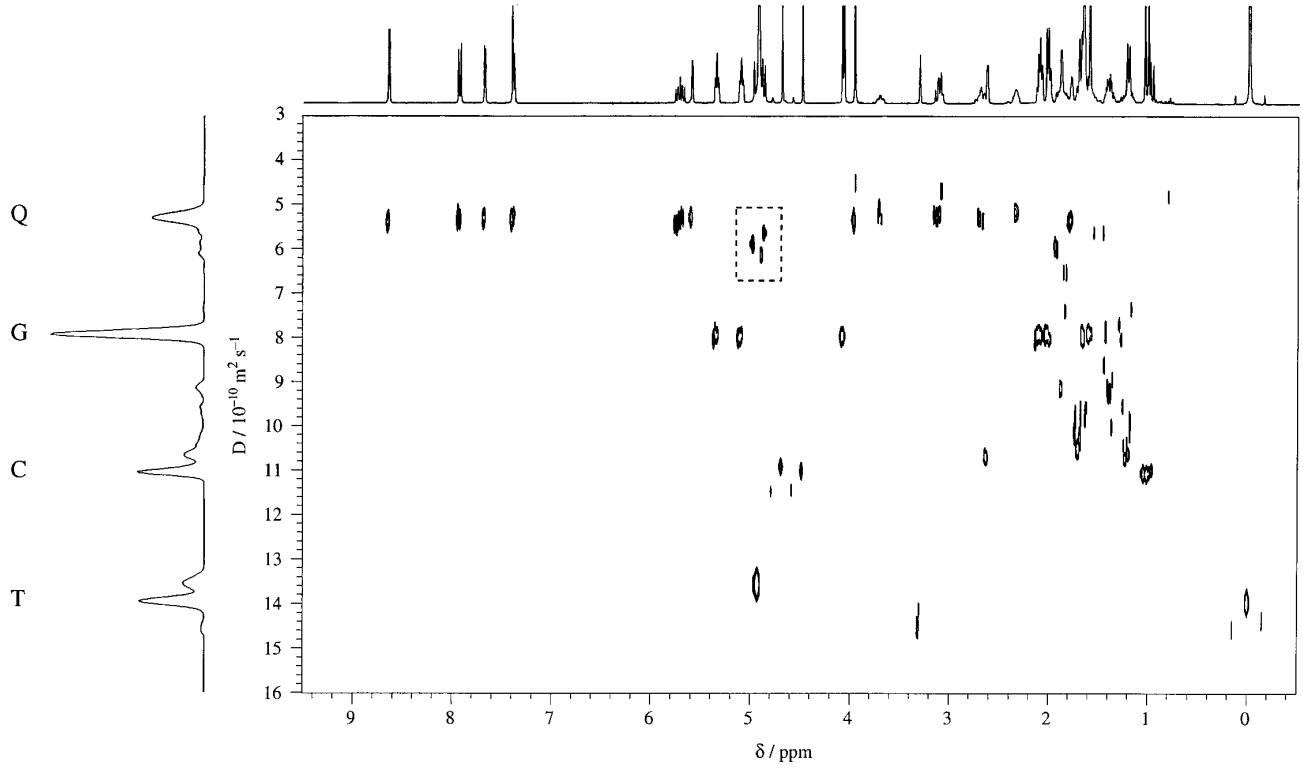

Figure 4. 400 MHz proton DOSY spectrum of the mixture used for Fig. 2, obtained using the gradient compensated stimulated echo GCSTESL sequence of Fig. 1(f), with (top) the normal 1D spectrum and (left) the integral projection of the DOSY spectrum on the diffusion axis. As with Fig. 3, the simple DOSY spectrum synthesis algorithm used makes no attempt to correct for experimental imperfections.

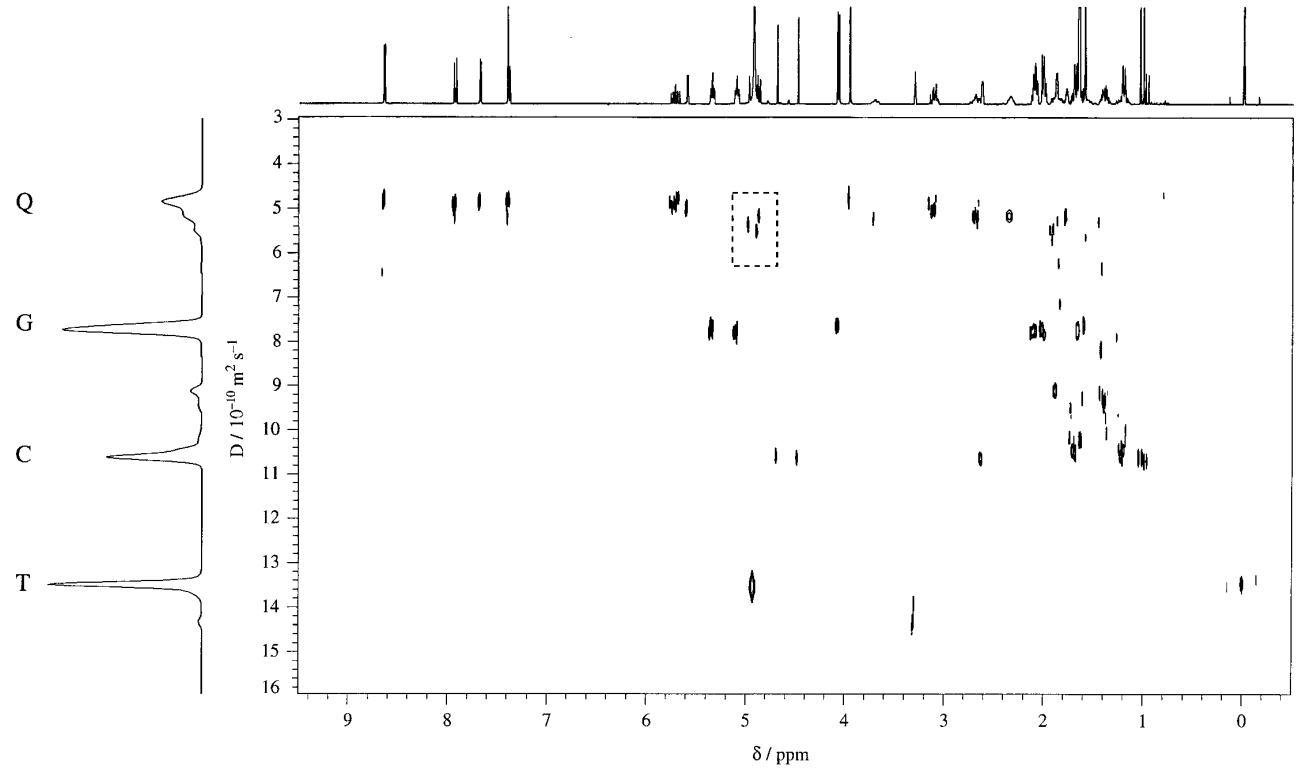

Figure 5. 400 MHz proton DOSY spectrum obtained from the GCSTESL data of Fig. 4, with (top) the normal 1D spectrum and (left) the integral projection of the DOSY spectrum on the diffusion axis. The DOSY spectrum synthesis algorithm used reference deconvolution and baseline correction to compensate for experimental imperfections, as described in the text. The boxed region around 4.9 ppm shows a reduction in systematic errors compared to the corresponding regions in Figs 3 and 4.

applied to all 10 spectra. The construction of the 2D DOSY spectrum then proceeded as before. In addition to the improvements made by using the gradient compensated pulse sequence with spin lock (GCSTESL), these data are much improved by the use of the FIDDLE algorithm[22] in correcting residual lineshape errors. The diffusion data obtained show small standard errors, giving a well defined diffusion projection with virtually no peaks appearing at intermediate diffusion values.

The effects of overlap in the NMR dimension on the distribution of signals in the diffusion dimension are illustrated by the region around 4.9 ppm, highlighted by dashed boxes in Figs 3–5, which contains a group of three quinine signals bracketing the residual water peak. The partial overlap between the quinine signals and the broad water signal adds a small, rapidly decaying component to the decay of the quinine signals with increasing gradient pulse area. Fitting the distorted decay with a single exponential as a function of gradient pulse area squared then gives an anomalously high estimate of the diffusion coefficient. As the lineshape of the water signal improves from Fig. 3 through to Fig. 5, so the extent of overlap between the skirts of the water signal and the quinine signals decreases and the quinine signals move back towards the correct diffusion coefficient.

A comparison of the TMS peaks in the three DOSY spectra is also instructive. As the accuracy of the diffusion data improves through the successive reduction in systematic errors between Fig. 3 and Fig. 5, the TMS peaks become narrower in the diffusion domain. Only in the final, baseline corrected spectrum do the ^{13}C satellites of the TMS signal appear at the same diffusion coefficient. This is a very stringent test of the quality of the data because of the high dynamic range involved (200 : 1): even a slight tilt in the baseline or a slight error in the phase of the parent signal will cause a large change in the apparent diffusion coefficients of the satellite signals.

Note added in proof. A BPPSTE sequence *has* been described previously, for studying electroosmotic flow: D. H. Wu, A. Chen and C. S. Johnson, *J. Magn. Reson. A* **115**, 123 (1995).

Acknowledgements

M.D.P. thanks Shell Research for a CASE studentship. The support of the EPSRC (grants GR/K16296, GR/K44619 and GR/L17443) is gratefully acknowledged, as is support from Pfizer Central Research, Sandwich. G.A.M. thanks the Leverhulme Trust for a Research Fellowship.

REFERENCES

1. K. F. Morris and C. S. Johnson, Jr, *J. Am. Chem. Soc.* **114**, 3139 (1992).
2. K. F. Morris and C. S. Johnson, Jr, *J. Am. Chem. Soc.* **115**, 4291 (1993).
3. E. O. Stejskal and J. E. Tanner, *J. Chem. Phys.* **42**, 288 (1965).
4. P. Stilbs, *Anal. Chem.* **53**, 2135 (1981).
5. D. P. Hinton and C. S. Johnson, Jr, *J. Phys. Chem.* **97**, 9064 (1993).
6. K. F. Morris, P. Stilbs and C. S. Johnson, Jr, *Anal. Chem.* **66**, 211 (1992).
7. D. Schulze and P. Stilbs, *J. Magn. Reson. A* **105**, 54 (1993).
8. D. H. Wu, W. S. Woodward and C. S. Johnson, Jr, *J. Magn. Reson. A* **104**, 231 (1993).
9. D. H. Wu, A. D. Chen and C. S. Johnson, Jr, *Anal. Chem.* **66**, 211 (1992).
10. H. Barjat, G. A. Morris, S. C. Smart, A. G. Swanson and S. C. R. Williams, *J. Magn. Reson. B* **108**, 170 (1995).
11. G. A. Morris and H. Barjat, in *Methods for Structure Elucidation by High Resolution NMR*, p. 209, edited by K. Köver and Gy. Batta, Elsevier, Amsterdam, 1997.
12. E. K. Gozansky and D. G. Gorenstein, *J. Magn. Reson. B* **111**, 94 (1996).
13. D. H. Wu, A. D. Chen and C. S. Johnson, *J. Magn. Reson. A* **121**, 88 (1996).
14. N. Birlirakis and E. Guittet, *J. Am. Chem. Soc.* **118**, 13083 (1996).
15. J. Ruiz-Cabello, G. W. Vuister, C. T. W. van Moonen, P. van Gelderen, J. S. Cohen and P. C. M. van Zijl, *J. Magn. Reson.* **100**, 282 (1992).
16. D. H. Wu, A. D. Chen and C. S. Johnson, *J. Magn. Reson. A* **123**, 215 (1996).
17. H. Barjat, G. A. Morris and A. G. Swanson, *J. Magn. Reson.* **131**, 131 (1998).
18. E. L. Hahn, *Phys. Rev.* **80**, 580 (1950).
19. H. Y. Carr and E. M. Purcell, *Phys. Rev.* **94**, 630 (1954).
20. K. Straubinger, F. Schick and O. Lutz, *J. Magn. Reson. B* **109**, 251 (1995).
21. P. Mansfield and B. Chapman, *J. Magn. Reson.* **66**, 573 (1986).
22. G. A. Morris, *J. Magn. Reson.* **80**, 547 (1988); G. A. Morris, H. Barjat and T. J. Horne, *Prog. Nucl. Magn. Reson. Spectrosc.* **31**, 197 (1997).
23. G. Wider, V. Dötsch and K. Wüthrich, *J. Magn. Reson. A* **108**, 255 (1994).
24. D. Wu, A. Chen and C. S. Johnson, Jr, *J. Magn. Reson. A* **115**, 260 (1995).
25. H. Barjat, P. B. Chilvers, B. K. Fetler, T. J. Horne and G. A. Morris, *J. Magn. Reson.* **125**, 197 (1997).
26. G. Bodenhausen, H. Kogler and R. R. Ernst, *J. Magn. Reson.* **58**, 370 (1984).

